

Resistance to freezing and thawing of mortar specimens made from sulphoaluminate–belite cement

I JANOTKA* and L' KRAJÈI

Institute of Construction and Architecture of the Slovak Academy of Sciences, Bratislava, Slovak Republic

MS received 3 June 2000; revised 2 September 2000

Abstract. Resistance to freezing and thawing of mortar specimens made from sulphoaluminate–belite cement (M–SAB) is compared with that of mortars made from portland cement (M–PC). The results suggest that larger median radius of the pores and total porosity of M–SAB compared to those of M–PC are primarily caused by the rapid setting of the SAB cement. The ‘coarsening’ of pore structure of mortar specimens under action of freezing and thawing is proved by the increase in the macropores portion, median pore radius, and total porosity values. This process is more intense in M–SAB. The effect of the frost attack is confirmed by lower compressive strength and dynamic modulus of elasticity on the one hand and higher absorption capacity, expansion, and crack propagation of M–SAB compared with those of M–PC on the other hand. Besides the decreased frost resistance of M–SAB as compared with that of M–PC, unsatisfactory passivation of steel in M–SAB was found. The reason of this fact is the pH value decrease to less than 11.5 of the M–SAB extract.

Keywords. Frost resistance; low-energy sulphoaluminate–belite cement; steel reinforcement corrosion.

1. Introduction

Portland cement (PC) production is markedly dependent on a relatively high thermal and electric energy consumption for firing and grinding of the clinker. Moreover, combustion of fossil fuels and decarbonation of limestone contribute to releasing up to $\sim 10^9$ t carbon dioxide into atmosphere annually (Mehta 1978). To solve these problems new alternative types replacing portland cements are developed. From this viewpoint sulphoaluminate–belite cements (SAB) represent one of the suitable and interesting tendencies in cement industry. The highest progress in SAB cements has been done in China and the UK (Wang *et al* 1992; Brooks and Sharp 1990).

The composition of Portland cement clinker comprises four phases: alite (C_3S), belite ($b-C_2S$), aluminate (C_3A), and ferrite (C_4AF). Typical PC clinker contains about 60–65% alite and 20–25% belite. In belite each mole of silica (SiO_2) is associated with two moles of lime (CaO). Belite is formed at 200°C lower temperature than alite (formed above 1400°C) and hence consumes less energy in its production than alite (Sahu and Majling 1994; Palou *et al* 1998). Calcium sulphoaluminate $C_4A_3\bar{S}$ often known as Klein’s compound is readily synthesized along with belite and ferrite at about 1300°C. The total theoretical heat requirement for SAB cement is 1337 kJ·kg⁻¹ compared with 1756 kJ·kg⁻¹ for PC (Janotka and Krajèi 1999). Enthalpy of formation for C_3S is 1848 kJ·kg⁻¹ clinker, for

$b-C_2S$ 1336 kJ·kg⁻¹ clinker, and that for $C_4A_3\bar{S}$ only around 800 kJ·kg⁻¹ clinker. Carbon dioxide release during firing of C_3S is 0.578 kg·kg⁻¹ clinker, of $b-C_2S$ 0.511 kg·kg⁻¹ clinker, and that of $C_4A_3\bar{S}$ is 0.216 kg·kg⁻¹ clinker (Sharp 1998). These data show that cements based on belite and sulphoaluminate are of great advantage from the view point of energy savings and quantity of CO_2 released during their production.

One productive approach to achieving a low energy cement is to incorporate a second reactive component along with belite. This component is $C_4A_3\bar{S}$ giving thus sulphoaluminate–belite cement (SAB). The major phases present in SAB cement are C_2S (usually below 30%), $C_4A_3\bar{S}$ (40–70%), a ferrite solid solution (10–35%), and gypsum (CS). A reduction in limestone utilization of about 40% and energy savings of 25% appear to be possible with high $C_4A_3\bar{S}$ contents. SAB cements can be made using industrial waste materials, notably fly ashes and gypsum, providing additional environmental advantages. The clinker is relatively easy to grind, giving a further saving in energy consumption. If manufactured on a large scale, SAB cements should be relatively cheap (Lawrence 1995).

Besides fly ash and gypsum, red mud and blastfurnace slag instead of natural materials can also be used for SAB cement production (Drábik and Petroviè 1985; Havlica *et al* 1993; Sahu *et al* 1993; Sahu and Majling 1993; Ali *et al* 1994).

The continuing problem of SAB cement is very short setting up to 45 min. Its durability under the attack of various media is still insufficiently verified (Beretka *et al*

*Author for correspondence

1993; Drábik *et al* 1996). Preliminary results show that SAB cement resistance to hydrochloric acid, sodium sulphate, and sodium chloride solutions is very similar to that of PC (Živica and Janotka 1996; Živica *et al* 1996).

Many serious causes of deterioration of concrete structures takes place under various environmental conditions. The action of frost belongs among the most significant. Concrete that is not resistant to freezing and thawing manifests two principal types of damage: internal cracking and surface scaling. Generally, freezing–thawing damage involves the expansion of cement paste generated by the 9% increase in volume as water is converted to ice inside a concrete element. Saturation of pores (91%) is necessary in some capillary cavities before cement paste will expand and crack on freezing. Therefore, the porosity of cement paste plays an important role in determining the

frost resistance of concrete. The cement paste may be frost resistant if the amount of freezable water is not large and if the air void system is proper, e.g. bubble spacing factor is 0.2 mm or less (Mehta *et al* 1992).

The manufacture of relatively cheap cements that are environmentally acceptable both in their production and use is very important contribution for concrete world. However, a lower firing temperature of SAB cement relative to that of portland cement is responsible for the production of cement of lower class. This current imperfection of SAB cements might not be the reason for discouraging from the next serious investigation. Therefore, one would put effort to make possible improvements in basic properties of SAB cements, and important engineering properties of SAB cement-based materials.

Many authors dealt with the problem of how to produce concrete that is durable when subjected to cycles of freezing and thawing. However, their attention was drawn mainly on concrete made from portland cement modified either by various solids or plasticizing and air-entraining admixtures. The objective of this paper is to investigate the frost resistance of cement based materials made from more and more low-energy SAB cement used in the world.

Table 1. Chemical composition of raw materials for SAB cement preparation.

| Component | Limestone (%) | Fly ash (%) | Gypsum (%) |
|--------------------------------|---------------|-------------|------------|
| Moisture | 0.10 | 0.35 | 1.23 |
| Ignition loss (1000°C) | 41.70 | 4.11 | 12.95 |
| SiO ₂ | 0.10 | 44.24 | – |
| Al ₂ O ₃ | 1.00 | 42.64 | 5.98 |
| Fe ₂ O ₃ | 0.15 | 4.18 | 1.89 |
| CaO | 55.36 | 2.80 | 25.84 |
| MgO | 1.40 | 0.75 | 0.63 |
| SO ₃ | – | – | 49.74 |
| Na ₂ O | 0.07 | 0.35 | 0.62 |
| K ₂ O | 0.03 | 0.52 | 1.09 |

2. Experimental

Ordinary portland cement and sulphoaluminate–belite cement were used in the experiment. Chemical composition of raw materials for SAB cement preparation is given in table 1. Chemical composition and properties of both cements are reported in table 2.

Table 2. Composition and properties of the cements employed.

| Component content (wt.%) | Ins. res. | SiO ₂ | CaO | Al ₂ O ₃ | Fe ₂ O ₃ | MgO | SO ₃ | Free CaO | Ign. loss |
|--------------------------|-----------|--|------------------|--------------------------------|--|-------------------|-----------------|----------|-----------|
| | | | | | | | | | |
| SAB | 1.35 | 19.69 | 52.58 | 15.45 | 2.60 | 1.50 | 6.12 | 0 | 0.48 |
| Cement | | Specific gravity (kg·m ⁻³) | | | Specific surface area (m ² ·kg ⁻¹) Blaine | | | | |
| PC | | 3313 | | | 397.9 | | | | |
| SAB | | 3246 | | | 381.0 | | | | |
| | | Content (Bogue) (%) | | | | | | | |
| | | C ₃ S | C ₂ S | C ₃ A | C ₄ AF | CaSO ₄ | | | |
| PC | | 56.6 | 17.5 | 7.6 | 11.5 | 4.5 | | | |
| | | Initial set (h/min) | | | Final set (h/min) | | | | |
| PC | | 3/10 | | | 5/05 | | | | |
| SAB | | 0/10 | | | 0/30 | | | | |
| | | pH of cement extract | | | | | | | |
| PC | | 12.55 | | | | | | | |
| SAB | | 11.84 | | | | | | | |

The mortars with cement to quartz sand (Standard STN 72 1208) ratio of 1 : 3 by mass and $w/c = 0.6$ (w = water, c = cement) were prepared. Fresh mixtures were compacted and moulded into $40 \times 40 \times 160$ mm prisms. The specimens were stored for 24 h in the moist air (100% R.H.) at 20°C and then kept in water for 27 days at the ambient temperature. After this basic curing one group of mortar specimens was still maintained under water and the second was subjected to freezing and thawing cycling (FTC). One cycle involved 6 h in water at $+20^\circ\text{C}$ and 18 h curing at -40°C . The specimens were exposed to frost during weekends. A Liebherr freezer from Austria was used for these tests. Visual observations of tested mortars were made periodically.

Mortar specimens were tested on dynamic modulus of elasticity (DME), flexural and compressive strength, and absorption capacity (AC). The test for AC was based on the difference in mass of the specimen saturated by water and dried at 105°C . The decrease in mass is calculated as % loss in mass.

Expansion of mortar specimens was measured by using a dilatometer apparatus with dial gauge. The gauge length was 100 mm with measuring accuracy of 0.001 mm. Changes in length were expressed in per mille.

Table 3. Clinker minerals in studied cements found by X-ray analysis.

| Cement | Clinker minerals | |
|--------|--|--|
| | Major | Minor |
| PC | C_3S , $\mathbf{b}\text{-C}_2\text{S}$ | C_3A , C_4AF |
| SAB | $\text{C}_4\text{A}_3\bar{\text{S}}$, $\mathbf{b}\text{-C}_2\text{S}$ | C_4AF |

Table 4. Strength and AC of mortars cured for 28 days in water.

| Mortar specimen | Strength (MPa) | | AC (wt.%) |
|-----------------|----------------|-------------|-----------|
| | Flexural | Compressive | |
| M-PC | 7.9 | 43.1 | 10.4 |
| M-SAB | 3.9 | 22.5 | 11.5 |

Table 5. Strength and AC of mortars at the time of FTC stopping.

| Mortar specimen | Curing | Strength (MPa) | | AC (wt.%) |
|-----------------|--------|----------------|-------------|-----------|
| | | Flexural | Compressive | |
| M-PC | Water | 9.1 | 54.2 | 9.5 |
| | FTC | 1.1 | 28.2 | 11.2 |
| M-SAB | Water | 4.5 | 24.0 | 11.4 |
| | FTC | 0.2 | 6.3 | 15.2 |

Pore structure of mortar specimens was studied by means of a high pressure mercury porosimeter model 2000 and macroporosimetry unit model 120 (both made by Erba Science in Milan, Italy). This apparatus enables estimation of pore radius between 3.75 nm and 0.2 mm.

The ability of mortars to protect steel was found by the potentiodynamic method (Standard STN 73 1341) in mortar extracts. The mortar extract was prepared according to above-mentioned standard as follows: the mortar specimens were crushed, ground (size of particles < 0.2 mm) and then mixed with distilled water (ratio 1 : 4). The prepared suspension was agitated for 6 h at the shaking machine. The water extract of mortar was obtained after filtration. The pH values of the extracts were estimated as well. For corrosion measurements reinforcing bars with diameter of 6 mm were used. Potentiodynamic curves of steel were obtained using Potentiostat OH-405 (Radelkis in Budapest, Hungary) under polarization rate $30 \text{ mV}\cdot\text{min}^{-1}$.

3. Results and discussion

Significant differences in chemical and phase composition, initial and final set between PC and SAB cement are shown in tables 2 and 3.

Flexural and compressive strengths of the mortar made from PC (M-PC) are higher than those of the mortar made from SAB cement (M-SAB). However, the value

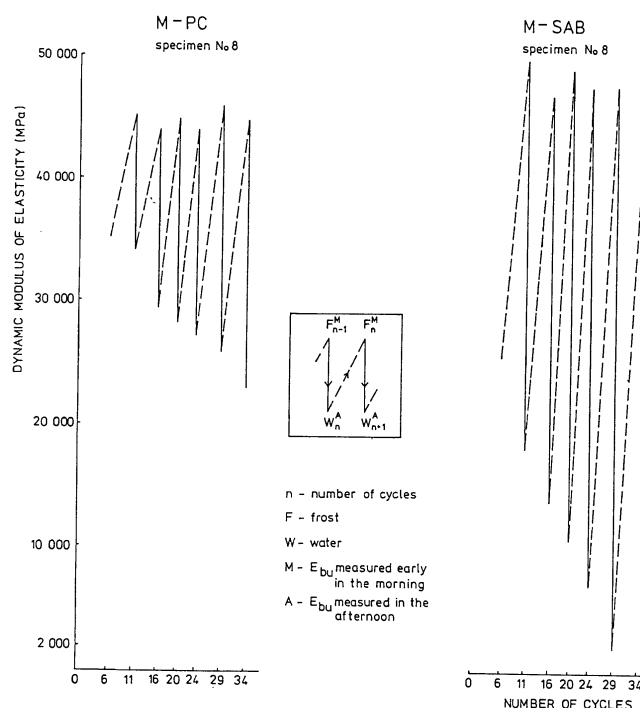


Figure 1. Decrease in DME of mortar specimens subjected to FTC.

of AC in M-SAB is partly higher in contrast to that of M-PC (table 4). Under FTC the decrease in compressive strength of M-SAB is more conspicuous than in M-PC. The increase in AC is evidently more considerable in M-SAB than in the M-PC (table 5). Under FTC the decrease in DME (figure 1) and increase in expansion (figure 2) are more pronounced in M-SAB than in M-PC. The FTC was stopped after 34 cycles when DME

decrease of M-SAB achieved 5% of the starting DME value. This value represents 29.2 GPa for M-SAB and 38.7 GPa for M-PC. When FTC was stopping, crack propagation was observed on the surface of M-SAB specimens (figure 3). By contrast a negligible crack propagation was found in M-PC specimens (figure 4). The frost resistance of M-SAB is lower than that of M-PC.

Table 6 shows the 'coarsening' of pore structure of the mortar specimens under FTC proved by the increase in macropores portion, median pore radius, and total porosity values. Significant differences in cumulative pore volume and pore radius distribution in M-PC and M-SAB are shown in figure 5. A larger pore volume with radius less than 800 nm was observed in M-PC opposite to M-SAB. This dependence is converse over pore radius values of 800 nm. The micropore radius distribution in tested mortars is decisively influenced by the used cement (coherence in course of curves 1 and 2 or 3 and 4 up to 800 nm and to a less extent in interval 800 nm-cca 5000 nm of pore radii). The effect of frost is distinctly manifested in the range of macropores when pore radius is over 7500 nm.

It is supposed that larger median pore radius and total porosity values in M-SAB in contrast to M-PC are primarily caused by rapid setting of the SAB cement. The process of periodical freezing and thawing is more conspicuous in M-SAB with coarser pore structure than that developed in M-PC. The effect of the frost attack is confirmed by compressive strength and DME and higher AC of M-SAB opposite to M-PC subjected to FTC.

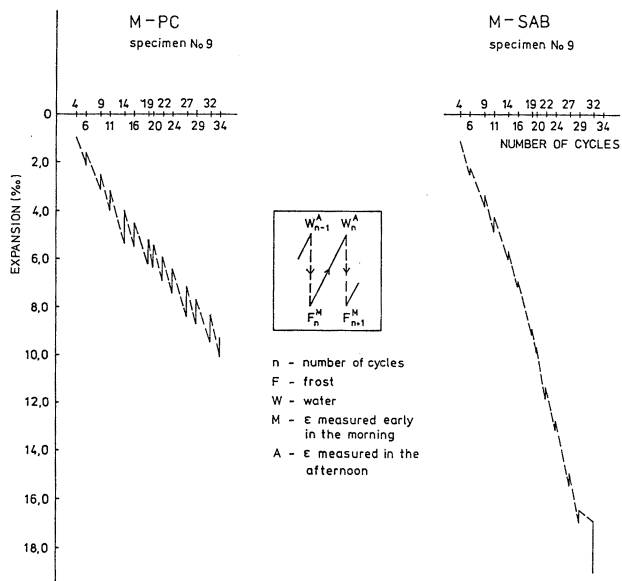


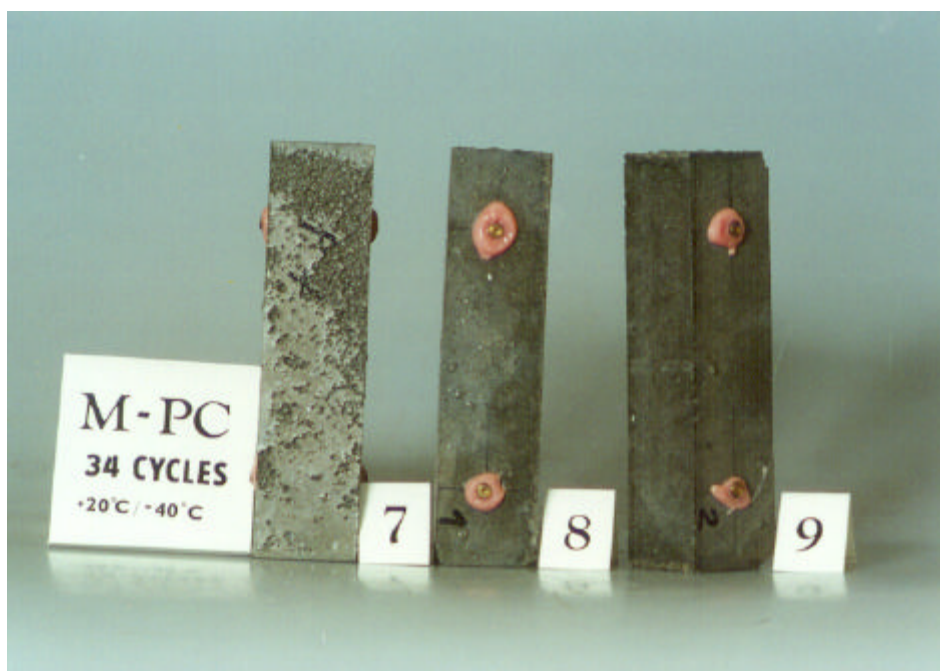
Figure 2. Increase in expansion of mortar specimens subjected to FTC.



Figure 3. Surface damage of M-SAB mortar specimens subjected to FTC.

Table 6. Pore structure study of tested mortars.

| Mortar specimen | Curing | Portion | | Median pore radius (nm) | Total porosity (%) |
|-----------------|--------|--------------------------|--------------------------|-------------------------|--------------------|
| | | Micropores < 7500 nm (%) | Macropores > 7500 nm (%) | | |
| M-PC | Water | 88.7 | 11.3 | 55.3 | 10.8 |
| | FTC | 79.7 | 20.3 | 184.9 | 14.7 |
| M-SAB | Water | 96.7 | 3.3 | 808.3 | 17.3 |
| | FTC | 85.4 | 14.6 | 1015.9 | 20.2 |

**Figure 4.** Surface damage of M-PC mortar specimens subjected to FTC.

The course of potentiodynamic curves of steel in M-SAB and M-PC extract (figure 6) as well as related values of basic reinforcement characteristics (table 7) indicate electrochemical state of steel. The passive zone is a part of the potention-dynamic curve with practically constant current density (figure 6). The presence of the protective oxide film on the steel surface is confirmed by the passive zone on the curve. However, the narrowing of the passive zone of steel in M-SAB extracts (figure 6) is the significant manifestation of the fact that steel is in non-stable passive state. The important electrochemical characteristic of steel—potential of breakdown—have dropped on values of 390 and 400 mV, respectively (table 7). Besides it is well known that $\alpha\text{-Fe}_2\text{O}_3$ protective oxide film on the steel surface starts to decompose below pH value of 11.5 (Gouda 1970) and subsequently steel is not fully passivated. Therefore, the worse ability of M-SAB to protect the steel against corrosion is caused by the pH

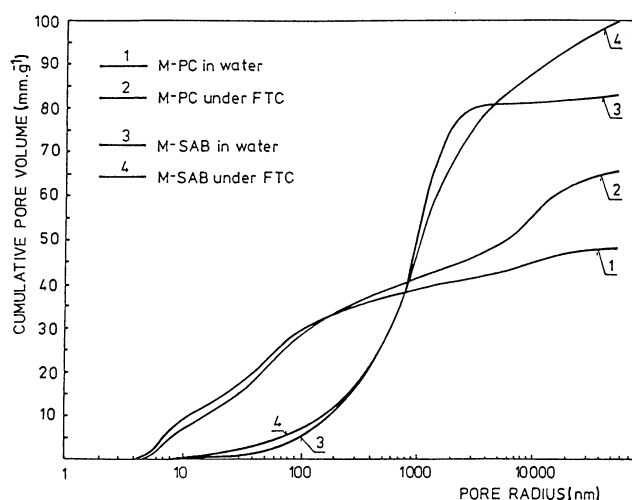
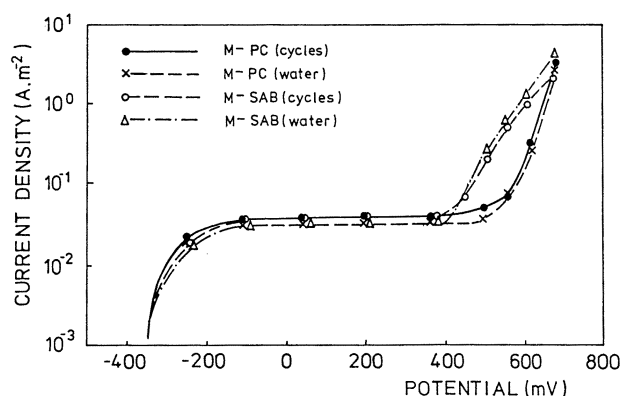
**Figure 5.** Cumulative pore volume versus pore radius in tested mortars.

Table 7. Test results of steel reinforcement corrosion of tested mortars.

| Mortar specimen | Curing | Stationary potential (mV) | Current density of passivation ($A \cdot m^{-2}$) | Potential of breakdown (mV) | State of steel | pH of extract |
|-----------------|--------|---------------------------|---|-----------------------------|--------------------|---------------|
| M-PC | Water | -345 | 0.031 | 560 | Passive | 12.37 |
| | FTC | -340 | 0.038 | 540 | Passive | 12.33 |
| M-SAB | Water | -340 | 0.030 | 400 | Non-stable-passive | 11.25 |
| | FTC | -345 | 0.036 | 390 | Non-stable-passive | 11.23 |

**Figure 6.** Potentiodynamic curves of steel immersed into M-SAB and M-PC extracts.

values decrease of its extract (11.23; 11.25) compared with that of M-PC extract (12.33; 12.37).

4. Conclusions

(I) Rapid initial set and different phase composition of SAB cement relative to those of portland cement contribute to the pore structure formation characterized by the extremely higher median pore radius and total porosity of M-SAB opposite to M-PC cured in water. These differences are more explicit at FTC. Higher drop in dynamic modulus of elasticity and compressive strength values as well as the increase in absorption capacity caused this.

(II) A more permeable pore system of M-SAB enables faster transfer of the larger volume of water throughout SAB cement mortars relative to those of M-PC. A growth of formed ice crystals is then the source of internal expansive stresses which are responsible for mortar deterioration.

(III) It is important to slow down the set of SAB cement by changes in raw meal and firing condition to produce cement of higher quality.

(IV) The primary reason of worsened ability of M-SAB to protect the steel against corrosion is the pH value

decrease to less than 11.5 of the mortar extract. It is necessary to provide increased alkalinity of SAB cement to avoid a danger of steel corrosion in SAB cement-based materials.

Acknowledgement

The authors are grateful to the Slovak Grant Agency for Science (Grant No. 2/7035/20) for support.

References

- Ali M, Gopal S and Handoo S K 1994 *Cem. Concr. Res.* **24** 715
- Beretka J, Santoro L, Sherman N and Valenti G L 1993 *Cem. Concr. Res.* **23** 1205
- Brooks S A and Sharp J H 1990 *Ettringite-based cements, calcium aluminate cements* (eds) R I Mangabhai and F N Spon (London) p. 335
- Drábik M and Petrovič J 1985 *Siliká ty* **29** 227
- Drábik M, Gáliková L and Slade R T C 1996 *Proceedings of MAETA workshop on high flexural polymer cement composite* (eds) N Maeda (Sakata: Maeta Concrete Industry Ltd) p. 107
- Gouda V K 1970 *Br. Corros. J.* **5** 198
- Havlica J, Roztocká D and Sahu S 1993 *Cem. Concr. Res.* **23** 294
- Janotka I and Krajčì L' 1999 *Adv. Cem. Res.* **11** 34
- Lawrence C D 1995 COPERNICUS Program Report CIPA-CT 94-0105 1-88
- Majling J, Sahu S, Vlna M and Roy D M 1993 *Cem. Concr. Res.* **23** 1351
- Mehta P K 1978 *World Cem. Tech.* 144
- Mehta P K, Schiessl P and Raupach M 1992 *Proceedings of 9th international congress on the chemistry of cement* (ed.) A K Mullick (New Delhi: National Council for Cement and Building Materials (NCB)) p. 571
- Palou M T, Majling J, Janotka I, Dan E and Popescu D 1998 *Ceramics* **42** 105
- Sahu S and Majling J 1993 *Cem. Concr. Res.* **23** 1331
- Sahu S and Majling J 1994 *Cem. Concr. Res.* **24** 1065

- Sahu S, Tomková V, Majling J and Havlica J 1993 *Cem. Concr. Res.* **23** 693
- Sharp J H 1998 *Proceedings of international conference on the cements for the future: Calcium sulfoaluminates* (London, Great Britain: The Institute of Materials and Society of Chemical Industry) p. 1
- STN 72 1208 Standard Testing Sands (in Czech)
- STN 73 1341 Standard Corrosion Protection of Reinforcements Provided by the Properties of Concrete. Methods of Test (in Slovak)
- Wang Y, Su M, Yang R and Lui B 1992 *Proceedings of 9th international congress on the chemistry of cement* (ed.) A K Mullick (New Delhi: National Council for Cement and Building Materials (NCB)) p. 454
- Živica V and Janotka I 1996 *Proceedings of Solid State Chemistry, Bratislava, Slovakia* (ed.) L T Nagy (Bratislava: The Slovak Society of Industrial Chemistry) p. 171
- Živica V, Janotka I and Majling J 1996 *Proceedings of the chemistry and microstructure of cement and concrete, Sheffield, UK* (ed.) F P Glasser (London: The Institute of Materials) Session 5